http://ansinet.com/itj

ITJ

ISSN 1812-5638

INFORMATION TECHNOLOGY JOURNAL

ANSInet
Asian Network for Scientific Information
308 Lasani Town, Sargodha Road, Faisalabad - Pakistan

Information Technology Journal 10 (7): 1395-1401, 2011
ISSN 1812-5638 / DOI: 10.3923/itj.2011.1395.1401

Inspection and Recognition of Generalized Surface Defect for Precise Optical Elements

[1,2]Hongyu Chu, [1]Zhijiang Xie, [3]Xu Xu, [3]Lidan Zhou and [1]Qin Liu
[1]The State Key Laboratory of Mechanical Transmission, Chongqing University, Chongqing 400030, China
[2]College of Information Engineering, Southwest University of Science and Technology, Mianyang, Sichuan 621010, China
[3]Laser Fusion Research Center, China Academy of Engineering Physics, Mianyang, Sichuan 621010, China

Abstract: According to the application of the current high-power solid-state laser devices with precision optical elements, it proposes the concept of the Generalized Surface Defects. Based on the machine vision, a non-contact detection scheme is proposed for the surface detection on defect features concerning the past low speed, smaller size in detection and less inconvenience in the testing or operation. A gantry platform for large-size three-dimensional motion and a clamping frame are designed, obtaining images with the linear array CCD, constructing partially closed spaces by the Graham method, achieving defective images through the adaptive threshold segmentation, extracting the defect parameters from the geometric space and the gray space and classifying the defects by the hierarchical support vector machine. Experiments show that the instrument detects the largest size of 700×600 mm and is capable of completing the scanning of the whole size of such elements within 25 min. Average error of area is 12% and average recognition accuracy is 92.2%.

Key words: Generalized surface defect, optical element, machine vision, threshold segmentation, support vector machine (SVM)

INTRODUCTION

Inertial Confinement Fusion (ICF) is taken as a very practical way of achieving a controlled fusion reaction to provide a solution to looming energy crisis. Coupled with its national defense military significance, ICF has been known as an important field of scientific research today. As the drive being most likely to achieve ICF, high-power solid-state laser driver has been a research focus (King, 2011; Stolz, 2007). At present, SHENGGUANG host which has been built in China is a huge high-power solid-state laser device composed of a large number of optical elements as well as mechanical and electrical elements. SHENGGUANG host's load capacity is an important indicator of the device. The results show that the surface defects and pollution residues of optical elements is one of the important factors for affecting the load capacity of high-power solid-state laser (Lidan *et al*., 2009).

In this study, the Generalized Surface Defect (GSD) are defined as the general term that includes pitting, scratches, broken edges, pollution residues and other existing surface damages, etc. In the past, the detection used to be done in a separate manner. The first is the surface defects, scratches, pitting and the similar injuries and the second category is the contaminated residues, mainly including solid particles, fiber and chemical pollution. For the former, the common detection methods (Xue *et al*., 2009) are visual inspection, comparison, adaptive Fourier filtering imaging, as well as angular spectral analysis, sampling of diffraction intensity and the machine vision. Visual inspection is a traditional method, where inspectors reply on the naked eyes or a magnifying glass to determine the level of defects based on their experience. The low-pass filter imaging principle involves the use of comparison to determine the defect size, where the target surface defects are compared with the reference standard, obtaining the equivalent width of the scratches or the equivalent diameters of the pitting. Adaptive Fourier filtering imaging shares the advantages of high-pass filter imaging. With a good filter effect, spatial modulator is able to correct the interference from the imaging of non-defects. As to smaller surface roughness, this method is available to achieve high accuracy. Angular spectrum utilizes the angular spectrum of scattered light to detect defective surface in their size and

Corresponding Author: Zhijiang Xie, The State Key Laboratory of Mechanical Transmission ,Chongqing University, Chongqing 400030, China

nature. Diffraction intensity sampling and analysis is applicable for detection of the scratch width, where the regular scratches of 2 ~ 30 μm in width may have a measurement error less than ± 15%. Dark-field scattering microscopy imaging method marks the realization of digital measurement on micro-level defects. Yang's teamwork, Xue's teamwork and Yong's teamwork, respectively, used machine vision to detect and classify the pitting and scratches (Yang *et al*., 2010; Xue *et al*., 2009; Yong *et al*., 2009). NIF has developed on-line advanced detector for detecting flaws (Conder *et al*., 2010).

Surface cleanliness is applied to the characterization of contaminated residue, which is inspected mainly by means of particle counting, IR, acoustic detection, color modulation and the detection that is based on machine vision. National Ignition Facility (NIF) introduced an indirect measurement method (Stowers, 1999) by which a specific cleaning solution is used to wash a certain area of precision optical surfaces, followed by using the filter paper to collect the solid particles contained in the used cleaning fluid and solid particles are thus obtained as an indirect indicator of the size and number of surface cleanliness. Infrared spectroscopy (Druy and Bolduc, 1999) is conducted by comparison between the actual detection of the optical element surface and the series of samples of different contaminants in terms of spectral density distribution of infrared light reflection, so as to determine the type and distribution of contaminants. Acoustic detection (Bilmes *et al*., 2005) requires the emission of the testing pulse YGA laser onto the surface, where the presence of particle contaminants may lead to the production of a specific frequency band of sound waves. Analysis of the wave may explore the corresponding particles in their size and distribution. Surface cleanliness testing method, based on machine vision, has aroused more and more concerns by researchers, for the use of scanning electron microscopy or atomic force microscope and other equipment may get nm even the sub-nm accuracy.

All of the above methods may be found with the following problems: First, the surface defect and surface contaminants are detected separately, without giving them a unified consideration. Second, the detection speed is slow, combined with a smaller detection size, the inconvenient operation or expensive equipment and so on. Third, the common recognition is often focused on pitting and scratches, without bringing the most common contaminant residues together for recognition. To solve practical problems, this paper proposes a non-contact detection that is based on machine vision and its corresponding recognition programs.

DETECTOR DESIGN

Figure 1 is a three-dimensional structure detector, where the motion platform and the clamping platform are parallel in a vertical structure, designed to prevent secondary pollution and also for easy loading and unloading. The motion platform works with special lubricant, but the up-and-down structure is still likely to have fall of the tiny contaminants. High-strength alloy is introduced to make the gantry structured clamping platform and motion platform, including three translation stage combinations to realize the free motion in an XYZ space. Translation stage is comprised of the ball screws, rolling rails and a base, being electrically controlled by highly differential stepper motors. The 1 μm linear scales are also included in the configuration, aiming at achieving closed-loop control to improve the movement accuracy.

The prototype system is varied in size specification of optical elements, with the maximum size up to 700× 600 mm. Contributed to scan movement, linear array CCD greatly increased the measurable area and thus improved the system scalability. Meanwhile, taking into account the cost factors in the same accuracy, the system is equipped with the CCD camera from DALSA which is featured with a higher resolution. The CCD linear array requires the uniform light spots and a higher light intensity. This results in the selection of halogen lamps with a high light intensity. Fiber transmission also comes in the parallel arrangement of fiber ends to get linear homogeneous spots. Dark-field illumination is there to highlight the outstanding and or depression features of the smooth surface defects.

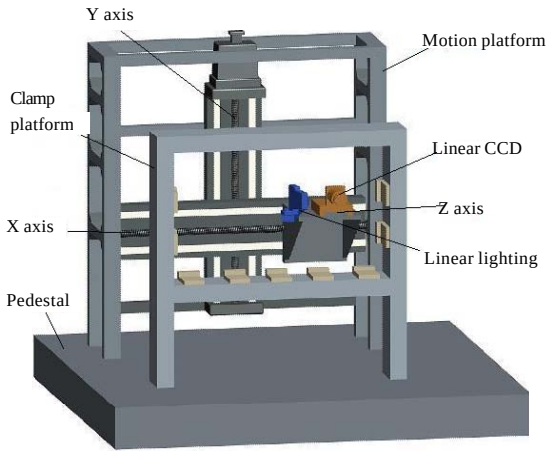

Fig. 1: Three-dimensional structure of the detector

IMAGE ACQUISITION

As the CCD camera is fixed onto the Z-axis motion platform, the image capture is actually the control process of platform movement and the CCD camera sampling. CCD camera imaging comes along the X axis, followed by splicing of the subgraphs obtained and finally to get the image of the entire optical surface. To ensure the data accuracy and reduce the scan time, the scanning system works in a snake pattern. Images from multiple scans are automatically spliced to complete the acquisition of the entire surface of a digital image. As indicated in Fig. 2, the shaded parts are the pictures scanned and the arrow line is the scanning trajectory. In the process of image acquisition, X-axis motion control is vital and required to be kept at a constant speed all the time. Acquisition interval must be kept away from both the acceleration and deceleration phases. The control curve of the stepper motor is shown in Fig. 3.

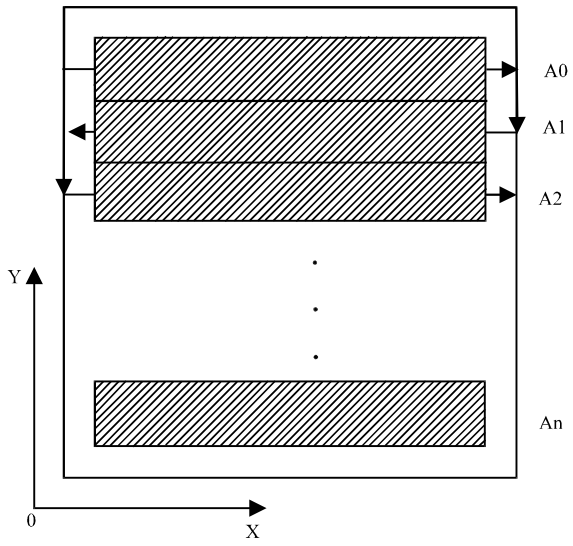

Fig. 2: Mode of the snake scan

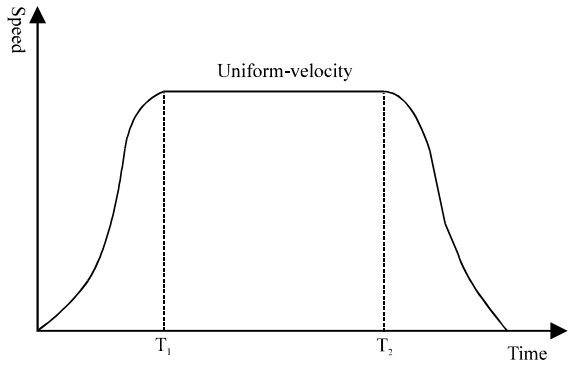

Fig. 3: Speed curve of the stepper motor

IMAGE PROCESSING

Under the influence of such factors as illumination, imaging, etc., images are often found with more texture and background interference. The key to image analysis lies in how to split the defects in the image from the background. In this study, the Canny operator is used for early detection of particle boundaries and then the Graham method is employed to construct a convex hull, where a partially closed area is formed for a single defect. Meanwhile, morphological dilation processing is performed and within the closed area, the defect image is obtained by means of segmentation. As a result, different thresholds are dynamically used for splitting the defects in an image.

Using canny operator to extract edge: As a local maximum edge detector, Canny operator is the most representative in edge detection. This operator acts to obtain an edge line pattern with better connection, in addition to the fine and complete edge depiction. Canny operator features better anti-noise performance and high positioning accuracy of the edge. This detection method involves the use of first derivative of Gaussian function, it can achieve a better balance between noise suppression and edge detection (Canny, 1986; Zhang *et al*., 2009; Zhou *et al*., 2010). Specific steps are as follows:

- With a Gaussian filter, image noise can be removed in image filtering. Two-dimensional Gaussian function using the first derivative is aimed to obtain smooth images to eliminate noise. Two-dimensional Gaussian function is shown in Eq. 1 as below:

$$G(x,y)=\frac{1}{2\pi\sigma^2}\left[-\left(\frac{x^2+y^2}{\sigma^2}\right)\right]^{\frac{1}{2}} \quad (1)$$

- The first derivative of Gaussian operators is called for image filtering, using Eq. 2 and 3 to get the size of each pixel gradient | G | and the direction:

$$|G|=\left[\left(\frac{\partial f}{\partial x}\right)^2+\left(\frac{\partial f}{\partial y}\right)^2\right]^{\frac{1}{2}} \quad (2)$$

$$\alpha=\tan^{-1}\left[\frac{\partial f}{\partial y}\Big/\frac{\partial f}{\partial x}\right] \quad (3)$$

- "Non-maxima suppression" of the image
- Dual-threshold method being employed to detect the connection edge. Regarding the possibly judged set

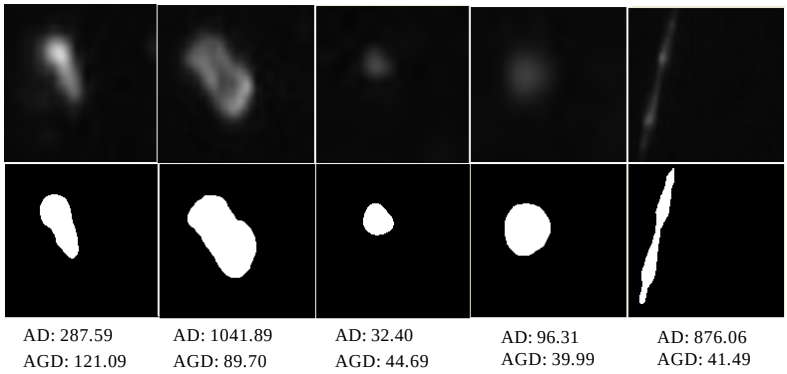

Fig. 4: Processing results of defects image, AD: Area of Defect, AGD: Average Gray of Defect

of edge points, the upper and lower limits are determined for the threshold. Non-maxima suppression images are treated with the upper limit to get a high threshold test image (T1) and a low threshold test image (T2). And then, the edge contours in the image T1 are connected. As the endpoint being connected, it finds the weak edge points in the image T2 to make up the gap edge of the image T1.

Construction of closed space for the extraction of defect feature: Edge extraction provides the location and contour of defects in the image, for being not often to get the edge of the closure and not appropriate for accurate segmentation. As for the edge being not closed, the traditional way may connect nearest-neighbor contacts to get a closed image .The problem also comes along: images with complex edges may be divided into multiple regions and have large errors on the image segmentation of surface defects. Convex hull is quite in the contrary, it contains perfect edges and the particle image information within. A convex set can be constructed by the Graham method. According to the statistic feature of the convexes, we use adaptive threshold segmentation to get the binary image. The total image is very big. Moreover, most of the defects on it are too small. In order to computer and analyze conveniently, we magnify the defect with the confine from 0.5 to 15. Defect Image results are as shown in Fig. 4. The Area of Defect (AD) is measured in μm^2.

CLASSIFICATION AND RECOGNITION

SHENGGUANG system performs its experiments using optical elements that were found with defects mainly including pitting, scratches and dust. Based on this, defect detection is determined in 3 categories: pitting, scratches and dust. Surface defect image is mainly characterized by the image pixels as to their geometric space, gray space and transform domain space. This paper presents the defect recognition in the study of the geometric space and gray space.

Geometrical parameters of defects are selected as follows: Length of the equivalent rectangular l_x, width l_y, convex tightness c_1, smoothness s, roundness r, area c_2 area tightness c_2, equivalent elongation e and overall curvature c_3. The total of 8 parameters combined presents a geometric description of spatial characteristics on defects. Nevertheless, these features are determined macroscopically and cannot describe the characteristics of defects in the edge line, nor in the image itself. Here, the mere geometrical parameters can be used as feature vectors, yet unavailable to distinguish all the defects. As a result, there is a need to consider the gray feature of defect images.

An effective tool for analysis of the gray space is Gray Level Co-occurrence Matrix (GLCM). GLCM is known as one of the statistical methods for analysis of texture, by which the image is calculated on the gray correlation between two points selected by a certain distance and a certain direction. The results reflect the statistical information on graphics regarding the direction, interval, amplitude and speed, thus providing accurate characterization on texture roughness and the repeating direction (Haralick *et al*.,1973; Mahi and Izabatene, 2011; Sheng *et al*., 2010). There are 6 common features parameters of GLCM, respectively: the energy E, entropy E, contrast C, uniformity H, correlation C and the inverse differential moment I, etc. Here, the energy parameter E is also called as Angular Second Moment (ASM), which is effective in measuring the distribution of defects on the uniformity of image intensity and texture thickness. For the defects with internal detailed texture, gray is evenly distributed and gets higher. Otherwise, it would be lower.

The SVM is a kind of effective machine learning methods to solve the nonlinear and high dimension problem with small sample set and it provides us with a new approach to recognize the defects (Benhaddouche and Benyettou, 2010). The process is following.

Selection of feature vector parameters: Pitting and dust are similar in imaging geometry, which is featured in round circular shapes or the like. Scratches and pitting are quite different from each other. The scratch area in the image has the length that is 4 times more than the width, along with a clear direction. There are also differences between pitting and dust imaging: dust imaging is reflected by its a better texture, pitting with a clear edge, yet inferior in texture features.

Based on the above analysis, the simple use of geometric parameters may distinguish scratches from other two types of features. As for distinguishing pitting and dust, gray space parameter is required. Thus, the system is designed with a two-stage SVM model: first, it divides the defects into scratch and non-scratch using the SVM_1, dividing the remaining defects into the categories of pitting and dust with SVM_2.

Of the geometric space parameters, l_x, l_y, r, e and c_3 are selected as the feature vector x of while the parameters and the energy of gray space parameters are selected as feature vector of . In SVM_1, the principal element analysis by dimension reduction is used to obtain a larger positive load for r and e. This shows that the roundness and elongation are the two parameters that contribute most to the defect geometric space. It is right these two parameters that function to draw a line between the linear scratches and other circular defects. As for SVM_2, only two parameters are there for classification, so there is no need to perform the Principal Component Analysis and the direct pattern recognition can be made.

Recognition: Both SVM1 and SVM2 are accompanied by Gaussian kernel (σ =2). Selection covers the 30 pitting samples, 30 dust samples and 20 scratch samples, plus another 10 samples prepared from a scratch sample database, to form a library of 30 training samples for each category. 30 samples are randomly selected as the test sample, which do not come from training samples. Recognition results are as shown in Table 1.

Based on the recognition results, the system is proven to have a higher rate of recognition on scratches. In actual operation, the system also shows a rate of detection up to 100% on scratches. The recognition on pitting and dust are a bit lower and particularly the false positive rate of regarding the dust as pitting is 13.4%. This explains the complexity of the dust imaging.

Table 1: Results of defect recognition

Type and number of defects	Recognition results			
	Scratch	Pitting	Dust	Others
Scratch (30)	30	0	0	0
Pitting (30)	0	27	3	0
Dust (30)	0	4	26	0
Recognition rate (%)	100	90	86.6	0

DISCUSSION

Visual inspection is applied in many occasions, but the method is involved with the subjective factors that may lead to low detection accuracy and inefficient. Comparison can be used to achieve the visual inspection purposes, but for smaller defects, less energy is scattered out of light, with the accuracy being strongly influenced by background light. To meet this situation, the only way is to get a substantial increase in imaging system magnification and accordingly, the targeted aperture is reduced. Adaptive fourier filtering imaging is attractive in the impact of background light to be reduced, only highlighted in the bright image of defects on the dark background. By the detection or observation of defect imaging concerning its extent of brightness and size, we can determine the size and nature of defects. Under the good effect of a spatial modulation filter, the interference from non-defects in bright imaging can well be excluded and in the case of smaller surface roughness, the method is able to provide a higher accuracy. As an indirect measurement, NIF merely works on detection of solid particle contamination, rather than other pollution residues. Infrared spectroscopy method brings about judgments on pollution residues with respect to its type and distribution, but slightly weak in the quantitative assessment. As for other methods, making the devices can be more complicated, much less the difficulties in quantitative evaluation.

Xue *et al.* (2009) developed a detection system for large diameter surface defects. The system can detect scratches and pitting but the efficiency is relatively low. Yong *et al.* (2009) introduced the area array CCD for measurement of surface defects, but being far apart between area array CCD and optical elements and complicated by light scattering, resulting in measurement error less than ideal. Yang *et al.* (2010) designed a measurement system based on area array CCD, available for measurement of scratches and pitting and also including the function of recognition. However, its small imaging area worsens the time-consuming measurement for large-diameter optical elements, requiring the processing efficiency to be improved. The detector in NIF is very intelligent and flexible. Our detector should be improved in these factors.

In contrast, first, the method proposed in this study is available to perform simultaneous detection on scratches, pitting and pollution residues and also to provide the quantitative evaluation of defects and contaminants on the surface. Second, due to the use of non-contact measurement, combined with a vertical motion platform and a clamping platform, the secondary pollution can be largely avoided. Third, the detection efficiency is higher, for the maximum diameter only needs less than 25 min.

Nonetheless, this detection device also shows several problems with it. First, installation and debugging are inconvenient in the first use. Motion platform and clamping platform should be riveted on the smooth pedestal and kept parallel. Second, accuracy of manufacture for the mechanical device is high. Third, an in-depth study of imaging mechanism for different defects, which may help us to improve the accuracy of detector, has not been done.

CONCLUSION AND FUTURE WORK

Aiming at the application of the high-power solid-state laser system works in larger sizes, this study proposed the novel concept of the Generalized Surface Defects (GSD), along with the development of a detection device based on the principle of machine vision, successfully achieving the detection on multiple-aperture optic elements. Regarding area of the defects tested, the contrast microscopy results showed an overall average error of 12%. At the same time, the support vector machine was also placed for the classification of major defects. The results show that the scratches and pits that are highly recognized, compared to the rate of recognition on the dust that needs to be improved, where further studies should be made on the imaging laws. In the next steps, our work will be focused on the following aspects: (1) To study the factors that cause system errors so as to further improve the accuracy of defect detection and classification. Especially it needs to study imaging mechanism of low gray small defect. (2) According to test results, research will be performed on how to describe the macro- evaluation of defects on the surface of the generalized optical elements, providing guidance for the SG-III works with optical elements.

ACKNOWLEDGMENTS

The work was supported by National Science Foundation of China and China Academy of Engineering Physics (Grant No. 10976034). The project's name is Macroscopic Description Method of Defect Model for Optical Element. This research project is conducted from Jan.1, 2010 to Dec.30, 2012.

REFERENCES

Benhaddouche, D. and A. Benyettou, 2010. The decision tree and support vector machine for the data mining. J. Applied Sci., 10: 1336-1340.

Bilmes, G.M., D.J.O. Orzi, O.E. Martinez and A. Lencina, 2005. New method for real-time surface cleanliness measurement. Proc. SPIE, 5856: 980-986.

Canny, J., 1986. A computational approach to edge detection. IEEE Trans. Patt. Anal. Mach. Intel., PAMI-8: 679-698.

Conder, A., J. Chang, L. Kegelmeyer, M. Spaeth and P. Whitman, 2010. Final Optics Damage Inspection (FODI) for the national ignition facility. Proc. SPIE, Vol. 7797. 10.1117/12.862596

Druy, M.A. and R.A. Bolduc, 1999. Fiber optic noncontact reflectance probe for detection of contamination in pharmaceutical mixing vessels. Proc. SPIE, 3538: 167-171.

Haralick, R.M., K. Shanmugam and I.H. Dinstein, 1973. Textural features for image classification. IEEE Trans. Syst. Man Cybernet., 3: 610-621.

King, J.J., 2011. Defense in depth: Laser safety and the national ignition facility. Proc. SPIE, Vol. 7916. 10.1117/12.879274

Lidan, Z., S. Jingqin, L. Lanqin, W. Wenyi, W. Fang, M. Lei, L. Ping and Z. Xiaomin, 2009. High power laser and particle beams. Opt. J., 21: 326-330.

Mahi, H., and H.F. Izabatene, 2011. Segmentation of satellite imagery using RBF neural network and genetic algorithm. Asian J. Applied Sci., 4: 186-194.

Sheng, X., P. Qi-Cong and H. Shan, 2010. An invariant descriptor design method based on MSER. Inform. Technol. J., 9: 1345-1352.

Stolz, C.J., 2007. The national ignition facility: The world's largest optical system. Proc. SPIE, Vol. 6834. 10.1117/12.773365

Stowers, I.F., 1999. Optical cleanliness specifications and cleanliness verification. Proc. SPIE, 3782: 525-530.

Xue, W., X. Zhijiang, S. Hongyan, C. Ping, 2009. Study on automatic flaw inspection system for large caliber precision optical surface. Chin. J. Sci. Instrum., 27: 1262-1265.

Yang, Y.Y., X. Gao, B. Xiao, D. Liu and Y.M. Zhuo, 2010. Optical microscopic imaging and digitized evaluation system for super-smooth surface defects. Infrared Laser Eng., 39: 325-329.

Yong, F., C. Niannian, G. Lingling, J. Yuan, W. Junbo, C. Xiaofeng, 2009. Digital detection system of surface defects for large aperture optical elements. High Power Laser Partic. Beams, 21: 1032-1036.

Zhang, B., L. Bai and X. Zeng, 2009. A novel subpixel edge detection based on the zernike moment. Inform. Technol. J., 9: 41-47.

Zhou, X.L., F.X. Yu, Y.C. Wen, Z.M. Lu and G.H. Song, 2010. Early fire detection based on flame contours in video. Inform. Technol. J., 9: 899-908.